Topological phases and quantum computation

A. Kitaev

California Institute of Technology, *Pasadena, CA 91125*

C. Laumann

Department of Physics, Princeton University, *Princeton NJ 08544*

OXFORD

UNIVERSITY PRESS

Contents

1

Introduction: The quest for protected qubits

The basic building block of quantum computation is the qubit, a system with two (nearly) degenerate states that can be used to encode quantum information. Real systems typically have a full spectrum of excitations that are considered illegal from the point of view of a computation, and lead to decoherence if they couple too strongly into the qubit states during some process. See Fig. 1.1. The essential problem then is to preserve the quantum state of the qubit as long as possible to allow time for computations to take place.

Assuming the gap Δ to the illegal states is reasonable, we can quite generally describe the dynamics of the qubit state by an effective Schödinger equation

$$\frac{d}{dt}|\Psi\rangle = -iH_{\text{eff}}|\Psi\rangle \tag{1.1}$$

where H_{eff} is the effective qubit Hamiltonian. In quantum optics, H_{eff} is often known with high precision. This is not so in condensed matter systems such as quantum dots. Even worse, H_{eff} may fluctuate or include interaction with the environment. This causes decoherence of the qubit state.

Ideally, we would like to arrange for H_{eff} to be zero (or $H_{\text{eff}} = \epsilon I$) for some good reason. Usually, we use a symmetry to protect degeneracies in quantum systems. For example, a quantum spin $\frac{1}{2}$ has a two-fold degeneracy protected by the $SU(2)$ symmetry, as do the $2s+1$ degeneracies of higher spins s. Indeed, any *non-Abelian* symmetry
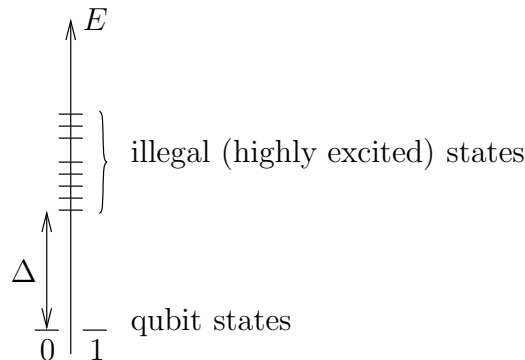

Fig. 1.1 Spectrum of a physical qubit system.

would work. Unfortunately, the $SU(2)$ symmetry of a spin is lifted by magnetic fields and it's generally difficult to get rid of stray fields.

Rather than symmetry, in what follows we will look to topology to provide us with physically protected degeneracies in quantum systems. In particular, we will examine a number of exactly solvable models in one and two dimensions which exhibit topologically phases – that is, gapped phases with a protected ground state degeneracy dependent on the topology of the manifold in which the quantum model is embedded. In Sec. 2 we warm up with the study of several quantum chains that exhibit Majorana edge modes and thus a two-fold degeneracy on open chains. The topological phenomena available in two dimensional models are much richer and will be the focus of the remaining three sections. We introduce and solve the toric code on the square lattice in Sec. 3, exhibiting its topolological degeneracy and excitation spectrum explicitly. The following section steps back to examine the general phenomenology of quasiparticle statistics braiding in two dimensional models. Finally, in Sec. 5 we introduce the honeycomb lattice model which exhibits several kinds of topological phases, including that of the simple toric code and, in the presence of time reversal symmetry breaking, a gapped phase with chiral edge modes protected by the topology of the Fermi surface.

2

Topological phenomena in 1D: boundary modes in the Majorana chain

We will consider two examples of 1D models with $\mathbb{Z}_2$ symmetry and topological degeneracy: the *transverse field Ising model* (TFIM) and the *spin-polarized superconductor* (SPSC). Although these models look rather different physically, we will find that they are mathematically equivalent and that they both exhibit a topological phase in which the ground state degeneracy is dependent on the boundary conditions of the chain. That is, the ground state on an open chain is 2-fold degenerate due to the presence of boundary zero modes, whereas the ground state is unique on a closed loop. This topological degeneracy will be stable to small *local* perturbations that respect the $\mathbb{Z}_2$ symmetry. More details on these models may be found in Kitaev (2000).

1. The *transverse field Ising model* is a spin-1/2 model with Hamiltonian:

$$H_S = -J \sum_{j=1}^{N-1} \sigma_j^x \sigma_{j+1}^x - h_z \sum_{j=1}^{N} \sigma_j^z. \tag{2.1}$$

Here J is the ferromagnetic exchange coupling in the x direction and h_z is a uniform transverse (z) field. This model has a $\mathbb{Z}_2$ symmetry given by a global spin flip in the σ_x basis:

$$P_S = \prod_{j=1}^{N} \sigma_j^z \tag{2.2}$$

2. The *spin-polarized 1-D superconductor* is a fermionic system with Hamiltonian:

$$H_F = \sum_{j=1}^{N-1} \left(-w(a_j^\dagger a_{j+1} + a_{j+1}^\dagger a_j) + \Delta a_j a_{j+1} + \Delta^* a_{j+1}^\dagger a_j^\dagger \right)$$

$$-\mu \sum_{j=1}^{N} \left(a_j^\dagger a_j - \frac{1}{2} \right) \tag{2.3}$$

where a_j and $a_j^\dagger$ are fermionic annihilation and creation operators, w is the hopping amplitude, Δ is the superconducting gap and μ is the chemical potential. For simplicity, we will assume that $\Delta = \Delta^* = w$, so that

$$H_F = w \sum_{j=1}^{N-1} (a_j - a_j^\dagger)(a_{j+1} + a_{j+1}^\dagger) - \mu \sum_{j=1}^{N} \left(a_j^\dagger a_j - 1/2 \right). \tag{2.4}$$

This model has a $\mathbb{Z}_2$ symmetry given by the fermionic parity operator:

$$P_F = (-1)^{\sum_j a_j^\dagger a_j} \tag{2.5}$$

Although the two models are mathematically equivalent, as we will see in Sec. 2.2, they are clearly physically different. In particular, for the superconductor, the $\mathbb{Z}_2$ symmetry of fermionic parity cannot be lifted by any local physical operator, as such operators must contain an even number of fermion operators. Unfortunately, for the spin system the degeneracy is lifted by a simple longitudinal magnetic field $h_x \sum_j \sigma_j^x$ and thus the topological phase of the TFIM would be much harder to find in nature.

2.1   Nature of topological degeneracy (spin language)

Consider the transverse field Ising model of Eq. (2.1). With no applied field, there are a pair of Ising ground states ($h_z = 0$):

$$|\psi_\rightarrow\rangle = |\rightarrow\rightarrow\rightarrow \cdots \rightarrow \rangle, \ |\psi_\leftarrow\rangle = |\leftarrow\leftarrow\leftarrow \cdots \leftarrow \rangle. \tag{2.6}$$

The introduction of a small field h_z allows the spins to flip in the σ^x basis. In particular, tunneling between the two classical ground states arises via a soliton (domain-wall) propagating from one side of the system to the other:

$$| \rightarrow\rightarrow\rightarrow \cdots \rightarrow \rangle \longrightarrow | \leftarrow:\rightarrow\rightarrow \cdots \rightarrow \rangle \longrightarrow | \leftarrow\leftarrow:\rightarrow \cdots \rightarrow \rangle \tag{2.7}$$

$$\longrightarrow | \leftarrow\leftarrow\leftarrow: \cdots \rightarrow \rangle \longrightarrow \cdots \longrightarrow | \leftarrow\leftarrow\leftarrow \cdots \leftarrow \rangle. \tag{2.8}$$

As usual, the tunneling amplitude t associated with this transition falls off exponentially in the distance the soliton must propagate

$$t \sim e^{-N/\xi} \tag{2.9}$$

where ξ is the correlation length of the model. The two-fold degeneracy is therefore lifted by the effective Hamiltonian:

$$H_{\text{eff}} = \begin{pmatrix} 0 & -t \\ -t & 0 \end{pmatrix}. \tag{2.10}$$

The splitting is exponentially small in the system size and the two-fold degeneracy is recovered in the thermodynamic limit as expected. Moreover, it is clear why introduction of a longitudinal field h_x will fully split the degeneracy.

2.2   Reduction of TFIM to SPSC by the Jordan-Wigner transformation

To show the equivalence of the one dimensional models introduced above, we will use a standard Jordan-Wigner transformation to convert the spins of the Ising model into

fermions. It is perhaps not surprising that a fermionic description exists for spin $1/2$ systems – we simplify identify the up and down state of each spin with the presence or absence of a fermion. The only difficulty arises in arranging the transformation so that the appropriate (anti)-commutation relations hold in each description. The Jordan-Wigner transformation does this by introducing string-like fermion operators that work out quite nicely in 1-D nearest neighbor models.

To reduce H_S to H_F, we

1. Associate the projection onto the z-axis of the spin with the fermionic occupation number:

$$| \uparrow \rangle \leftrightarrow n = 0, \quad | \downarrow \rangle \leftrightarrow n = 1. \tag{2.11}$$

That is,

$$\sigma_j^z = (-1)^{a_j^\dagger a_j}. \tag{2.12}$$

2. Introduce the string-like annihilation and creation operators

$$a_j = \left(\prod_{k=1}^{j-1} \sigma_k^z \right) \sigma_j^+$$

$$a_j^\dagger = \left(\prod_{k=1}^{j-1} \sigma_k^z \right) \sigma_j^- \tag{2.13}$$

where σ^+ and σ^- are the usual spin raising and lower operators. At this stage, we can check that the usual fermionic anticommutation relations hold for the $a_j, a_j^\dagger$:

$$\left\{ a_i, a_j^\dagger \right\} = \delta_{ij} \tag{2.14}$$

3. Observe that

$$\sigma_j^x \sigma_{j+1}^x = -(a_j - a_j^\dagger)(a_{j+1} + a_{j+1}^\dagger), \tag{2.15}$$

so H_S (Eq. (2.1)) reduces to H_F (Eq. (2.4)) with

$$w = J, \quad \mu = -2h_z \tag{2.16}$$

2.3 Majorana operators

Majorana operators provide a convenient alternative representation of Fermi systems when the number of particles is only conserved modulo 2, as in a superconductor. Given a set of N Dirac fermions with annihilation/creation operators $a_j, a_j^\dagger$, we can define a set of $2N$ real Majorana fermion operators as follows:

$$c_{2j-1} = a_j + a_j^\dagger$$

$$c_{2j} = \frac{a_j - a_j^\dagger}{i}. \tag{2.17}$$

These operators are Hermitian and satisfy a fermionic anticommutation relation:
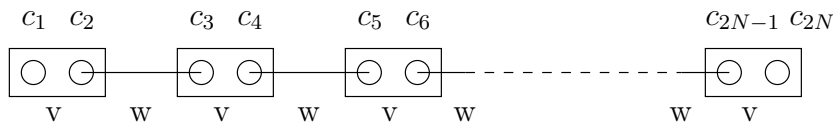
$$c_k^\dagger = c_k$$

Fig. 2.1 Majorana chain representation of 1-d superconductor. Each boxed pair of Majoranas corresponds to one site of the original fermionic chain.

$$c_k^2 = 1, \quad c_k c_l = -c_l c_k (k \neq l). \tag{2.18}$$

Or, more compactly,

$$\{c_k, c_l\} = 2\delta_{kl}. \tag{2.19}$$

From any pair of Majorana operators, we can construct an annihilation and creation operator for a standard Dirac fermion ($a = (c_1 + ic_2)/2$ and h.c.), and thus the unique irreducible representation for the pair is a 2-dimensional Hilbert space which is either occupied or unoccupied by the a fermion.

Both models H_S and H_F can be written as

$$H_{\mathrm{maj}} = \frac{i}{2} \left(v \sum_{j=1}^{N} c_{2j-1} c_{2j} + w \sum_{j=1}^{N-1} c_{2j} c_{2j+1} \right) \tag{2.20}$$

where $v = h_z = -\mu/2$ and $w = J$. The $\mathbb{Z}_2$ symmetry of fermionic parity is given in the Majorana language by

$$P_{\mathrm{maj}} = \prod_{k=1}^{N} (-ic_{2k-1} c_{2k}). \tag{2.21}$$

We can view this model graphically as a chain of coupled Majorona modes, two to each of the N sites of the original problem as in Fig. 2.1. If $v = 0$, then the Majorana modes at the ends of the chain are not coupled to anything. This immediately allows us to identify the 2-fold ground state degeneracy in H_{maj} as the tensor factor given by the 2-dimensional representation of the boundary pair c_1, c_{2N}.

We will see in Sec. 2.4 that if $v \neq 0$ but $|v| < w$, the operators c_1 and c_{2N} are replaced by some *boundary mode operators* b_l, b_r. The effective Hamiltonian for this piece of the system is then

$$H_{\mathrm{eff}} = \frac{i}{2} \epsilon b_l b_r = \epsilon (a^\dagger a - \frac{1}{2}) \tag{2.22}$$

where $\epsilon \sim e^{-N/\xi}$ and a, $a^\dagger$ are the Dirac fermion operators constructed from the boundary pair. Thus, the ground state degeneracy is lifted by only an exponentially small splitting in system size.

2.4 General properties of quadratic fermionic Hamiltonians

We now step back and consider a generic quadratic fermionic Hamiltonian:

$$H(A) = \frac{i}{4} \sum_{j,k} A_{jk} c_j c_k \tag{2.23}$$

where A is a real, skew-symmetric matrix and the c_j are Majorana fermion operators. The normalization $\frac{i}{4}$ is convenient because it has the property that

$$[-iH(A), -iH(B)] = -iH([A, B]) \tag{2.24}$$

where $A, B \in \mathfrak{so}(2N)$, and $H(A), H(B)$ act on the Fock space $\mathfrak{F}_N = \mathbb{C}^{2^N}$. Thus $H(\cdot)$ provides a natural representation of $\mathfrak{so}(2N)$.

We now bring $H(A)$ to a canonical form:

$$H_{\text{canonical}} = \frac{i}{2} \sum_{k=1}^{m} \epsilon_k b_k' b_k'' = \sum_{k=1}^{m} \epsilon_k (\tilde{a}_k^\dagger \tilde{a}_k - \frac{1}{2}) \tag{2.25}$$

where b_k', b_k'' are appropriate real linear combinations of the original c_j satisfying the same Majorana fermion commutation relations and the $\tilde{a}_k, \tilde{a}_k^\dagger$ are the annihilation and creation operators associated to the b_k', b_k'' pair of Majoranas. This form for H follows immediately from the standard block diagonalization of real skew symmetric matrices

$$A = Q \begin{pmatrix} 0 & \epsilon_1 & & & \\ -\epsilon_1 & 0 & & & \\ & & 0 & \epsilon_2 & \\ & & -\epsilon_2 & 0 & \\ & & & & \ddots \end{pmatrix} Q^T, \quad Q \in O(2N), \epsilon_k \geq 0 \tag{2.26}$$

From this form it is easy to check that the eigenvalues of A are $\pm i\epsilon_k$ and that the eigenvectors are the coefficients of c in $\tilde{a}_k, \tilde{a}_k^\dagger$.

If some of the ϵ_k vanish, then we refer to the associated fermions as *zero modes*. In particular, these will lead to ground state degeneracies, since occupation or nonoccupation of such modes does not affect the energy. For the Majorana chain of Eq. (2.20), we have

$$A = \begin{pmatrix} 0 & v & & & \\ -v & 0 & w & & \\ & -w & 0 & v & \\ & & -v & 0 & w \\ & & & -w & 0 \\ & & & & & \ddots \end{pmatrix} \tag{2.27}$$

We can find a vector u such that $uA = 0$ by inspection:

$$u = (1, 0, \frac{v}{w}, 0, \left(\frac{v}{w}\right)^2, 0, \cdots) \tag{2.28}$$

This vector leads to a left boundary mode

$$b_l = \sum u_k c_k \tag{2.29}$$

while an analogous calculation starting at the right end will find a right boundary mode b_r. These modes form a Majorana canonical pair, leading to a two-fold degeneracy of the ground state of the chain. Clearly, $u_k \sim e^{-k/\xi}$ falls off exponentially from the edges of the chain with correlation length $\xi^{-1} = \ln \left| \frac{w}{v} \right|$, as expected in section 2.3.

2.5   Why are the boundary modes robust?

In the simple case of a quadratic fermion Hamiltonian, we know that the modes correspond to eigenvalues of a skew-symmetric real matrix. These come in pairs $\pm i\epsilon$, in general, and the case $\epsilon = 0$ is special. In particular, if the pair of Majoranas corresponding to a zero mode are physically well separated, we expect perturbations to have trouble lifting the boundary degeneracy.

More generally, for interacting fermions, we can extend the symmetry group $\mathbb{Z}_2$, generated by $P = P_{\mathrm{maj}}$, to a *non-commuting* algebra acting on the the ground state space $\mathfrak{L}$. First, in the noninteracting limit, at $v = 0$, we define

$$X = Y \prod_{k=1}^{j} (-ic_{2k-1}c_{2k}) \tag{2.30}$$

where $Y = c_{2j+1}$ is a local Majorana operator at site $2j + 1$. A straightforward calculation shows that

$$XP = -PX \tag{2.31}$$

and that $[H, X] = 0$ so that the algebra generated by X, P acts on $\mathfrak{L}$ nontrivially. We now allow Y to vary as we adiabatically turn on interactions and, so long as an energy gap is maintained, we expect Y to remain a local operator near $2j$, which we can separate from the boundary by suitably large choice of j. That is, to find Y, one needs to know the ground state or at least the structure of the ground state near $2j$. This is a nontrivial operation but see Hastings and Wen (2005) for more details.

3
The two-dimensional toric code

The toric code is an exactly solvable spin $1/2$ model on the square lattice. It exhibits a ground state degeneracy of 4^g when embedded on a surface of genus g and a quasiparticle spectrum with both bosonic and fermionic sectors. Although we will not introduce it as such, the model can be viewed as an Ising gauge theory at a particularly simple point in parameter space (see Sec. 4.5). Many of the topological features of the toric code model were essentially understood by Read and Chakraborty (1989), but they did not propose an exactly solved model. A more detailed exposition of the toric code may be found in Kitaev (2003).

We consider a square lattice, possibly embedded into a nontrivial surface such as a torus, and place spins on the edges, as in Fig. 3.1. The Hamiltonian is given by

$$H_T = -J_e \sum_s A_s - J_m \sum_p B_p \qquad (3.1)$$

where s runs over the vertices (stars) of the lattice and p runs over the plaquettes. The star operator acts on the four spins surrounding a vertex s,
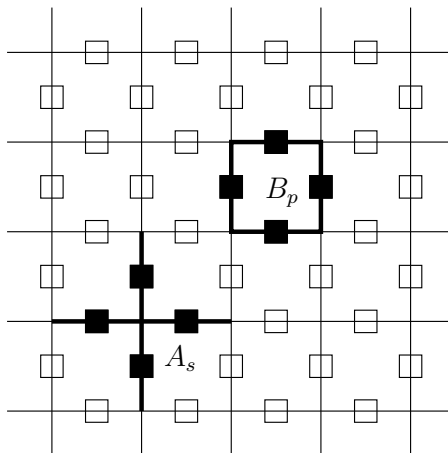

Fig. 3.1 A piece of the toric code. The spins live on the edges of the square lattice. The spins adjacent to a star operator A_s and a plaquette operator B_p are shown.

$$A_s = \prod_{j \in \text{star}(s)} \sigma_j^x \tag{3.2}$$

while the plaquette operator acts on the four spins surrounding a plaquette,

$$B_p = \prod_{j \in \partial p} \sigma_j^z. \tag{3.3}$$

Clearly, the A_s all commute with one another, as do the B_p. Slightly less trivially,

$$A_s B_p = B_p A_s \tag{3.4}$$

because any given star and plaquette share an even number of edges (either none or two) and therefore the minus signs arising from the commutation of σ^x and σ^z on those edges cancel. Since all of the terms of H_T commute, we expect to be able to solve it term by term.

In particular, we will solve H_T working in the σ^z basis. Define classical variables $s_j = \pm 1$ to label the σ^z basis states. For each classical spin configuration $\{s\}$, we can define the plaquette flux

$$w_p(s) = \prod_{j \in \partial p} s_j. \tag{3.5}$$

If $w_p = -1$, we say that there is a *vortex* on plaquette p.

3.1 Ground states

To find the ground states $|\Psi\rangle$ of H_T, we need to minimize the energy, which means maximize the energy of each of the A_s and B_p terms. The plaquette terms provide the condition

$$B_p|\Psi\rangle = |\Psi\rangle \tag{3.6}$$

which holds if and only if

$$|\Psi\rangle = \sum_{\{s : w_p(s) = 1 \ \forall p\}} c_s |s\rangle \tag{3.7}$$

. That is, the ground state contains no vortices. The group of star operators act on the configurations s by flipping spins. Thus, the star conditions

$$A_s|\Psi\rangle = |\Psi\rangle \tag{3.8}$$

hold if and only if *all of the c_s are equal for each orbit of the action of star operators*. In particular, if the spin flips of A_s are ergodic, as they are on the plane, all c_s must be equal and the ground state is uniquely determined.

On the torus, the star operators preserve the *cohomology class* of a vortex-free spin configuration. In more physical terms, we can define conserved numbers given by the Wilson loop like functions

$$w_l(s) = \prod_{j \in l} s_j, \quad l = l_1, l_2 \tag{3.9}$$

where l_1 and l_2 are two independent non-trivial cycles on the square lattice wrapping the torus (Fig. 3.2). Any given star will overlap with a loop l in either zero or two
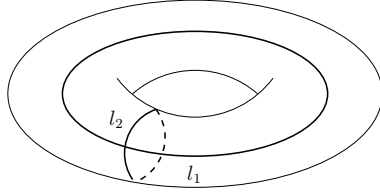
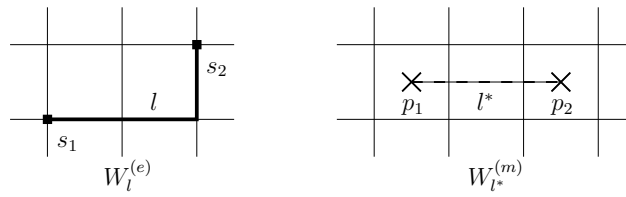**Fig. 3.2** Large cycles on the torus.

Fig. 3.3 Electric and magnetic path operators.

edges and therefore A_s preserves w_l. Since there are two independent loops on the torus, each of which can have $w_l = \pm 1$, there is a four-fold degenerate ground state:

$$|\Psi\rangle = \sum_{\{s:w_p(s)=1 \ \forall p\}} c_{w_{l_1} w_{l_2}} |s\rangle. \tag{3.10}$$

3.2 Excitations

The excitations of the toric code come in two varieties: the *electric charges* and *magnetic vortices* of a $\mathbb{Z}_2$ gauge theory. We will see this connection more explicitly later. In the following, we restrict attention to the planar system for simplicity.

To find the electric charges, let us define the electric path operator

$$W_l^{(e)} = \prod_{j \in l} \sigma_j^z \tag{3.11}$$

where l is a path in the lattice going from s_1 to s_2 (see Fig. 3.3). This operator clearly commutes with the plaquette operators B_p and with all of the star operators A_s except for at the end points s_1 and s_2, where only one edge overlaps between the star and the path and we have

$$W_l^{(e)} A_{s_1} = -A_{s_1} W_l^{(e)}. \tag{3.12}$$

Therefore, the state

$$|\Psi_{s_1,s_2}\rangle = W_l^{(e)} |\Psi_0\rangle, \tag{3.13}$$

where $|\Psi_0\rangle$ is the planar ground state, is an eigenstate of the Hamiltonian with excitations (charges) at s_1 and s_2 that each cost energy $2J_e$ to create relative to the ground state.

An analogous construction will find the magnetic vortices: we can define a dual path operator

$$W_{l^*}^{(m)} = \prod_{j \in l^*} \sigma_j^x \tag{3.14}$$

where the path l^* lies in the dual lattice (see Fig. 3.3) and goes from p_1 to p_2. In this case, the stars A_s all commute with $W_{l^*}^{(m)}$, as do all of the plaquette operators B_p except the two at the end points of l^*, which anticommute. Thus, the $W_{l^*}^{(m)}$ operator creates a pair of magnetic vortices on the plaquettes p_1 and p_2 at an energy of $2J_m$ each.

4

Abelian anyons and quasiparticle statistics

Let us discuss what can possibly happen if we exchange two particles in two dimensions. To ensure that particle statistics is well-defined, we assume that there is no long-range interaction and that the phase is gapped. If we drag two particles around one another adiabatically,

Top View   Side View

then we expect both dynamical phase accumulation and a statistical effect due to the exchange. We are well acquainted with this effect for everyday bosons and fermions, for which:

$$\begin{aligned} \text{Bosons:} \quad & |\Psi\rangle \mapsto |\Psi\rangle \\ \text{Fermions:} \quad & |\Psi\rangle \mapsto -|\Psi\rangle \end{aligned} \tag{4.1}$$

where we have dropped the dynamical phase so as to focus on the statistics. In both of these standard cases, a full rotation (two exchanges),

Top View   Side View

leaves $|\Psi\rangle$ unchanged.

In principle,

$$R_{ab} = \tag{4.2}$$

is an arbitrary phase factor or even an operator (*braiding operator*). If the two particles are distinguishable ($a \neq b$), then R_{ab} does not have an invariant meaning, but the *mutual statistics*

$$R_{ba} \cdot R_{ab} = \text{(figure)}$$

$$\begin{matrix} a & b \end{matrix}$$

(4.3)

does.

Let us illustrate this in the toric code model. In section 3.2 we found two kinds of quasiparticle excitations in the toric code: electric charges (e) and magnetic vortices (m). Since path operators of the same type commute with one another, it is easy to show that each of these are bosons. However, they have nontrivial mutual statistics.

To calculate the mutual statistics, consider taking a charge e around a vortex m.
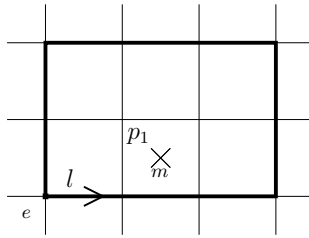
Let $|\xi\rangle$ be some state containing a magnetic vortex at p_1. Under the full braiding operation,

$$|\xi\rangle \mapsto \left(\prod_{j \in l} \sigma_j^z \right) |\xi\rangle$$

$$= \left(\prod_{p \text{ inside } l} B_p \right) |\xi\rangle$$

(4.4)

where the second line is a Stokes' theorem like result relating the product around a loop to the products of internal loops. Since

$$B_{p_1} |\xi\rangle = -|\xi\rangle$$

(4.5)

for the plaquette p_1 containing the vortex, we have that

$$|\xi\rangle \mapsto -|\xi\rangle,$$

(4.6)

or

$$\begin{matrix} e & m \end{matrix} \qquad \qquad \begin{matrix} e & m \end{matrix}$$

$$\text{(figure)} = - \text{(figure)}$$

$$\begin{matrix} e & m \end{matrix} \qquad \qquad \begin{matrix} e & m \end{matrix}$$

(4.7)

Using the bosonic self-statistics equations,

$$
\begin{array}{cccc}
e & e & e & e \\
\end{array}
\qquad
\begin{array}{cccc}
m & m & m & m \\
\end{array}
$$

(4.8)

we can derive the nontrivial corollary that composite $e - m$ particles are fermions:

$$
\tag{4.9}
$$

4.1   Superselection sectors and fusion rules

Initially, we exhibited two kinds of bosonic excitations in the toric code model (charges e and vortices m) in the solution of the Hamiltonian. After a bit of work, we discovered that a composite $e - m$ object has a meaningful characterization within the model as well, at least in that it has fermionic statistics. This begs the question, how many particle types exist in the toric code model and how can we identify them?

We take an algebraic definition of a particle type: each type corresponds to a *super-selection sector*, which is a representation of the local operator algebra. In particular, we say that two particles (or composite objects) are *of the same type*

$$
a \sim b \tag{4.10}
$$

if a can be transformed to b by some operator acting in a finite region. For example, in the toric code, two e-particles are equivalent to having no particles at all,

$$
\tag{4.11}
$$

by acting with an appropriate, geometrically bounded electric path operator $W_l^{(e)}$.

We introduce the notation

$$
e \times e = 1 \tag{4.12}
$$

to represent the *fusion rule* that two e-particles are equivalent to the vacuum sector 1. In the toric code, there are 4 superselection sectors:

$$
1, \ e, \ m, \ \text{and} \ \epsilon = e \times m \tag{4.13}
$$

with the fusion rules:

$$
\begin{aligned}
e \times e &= 1 & e \times m &= \epsilon \\
m \times m &= 1 & e \times \epsilon &= m \\
\epsilon \times \epsilon &= 1 & m \times \epsilon &= e
\end{aligned}
\tag{4.14}
$$

4.2   Mutual statistics implies degeneracy on the torus

This is an argument due to Einarsson (1990). Suppose that there are at least two particle types, e and m with -1 mutual statistics. Let us define an operator Z acting on the ground state in an abstract fashion (not refering to the actual model) which creates an e pair, wraps one particle around the torus and annihilates the pair. In the toric code, this will be the path operator $W_l^{(e)} = \prod_{j \in l} \sigma_j^z$ for a loop l winding one of the nontrivial cycles on the torus, but we need not know that specifically.

We can define another operator X that creates a pair of the other type m and winds around the other nontrivial cycle on the torus. But now a bit of geometric introspection reveals that the combination,

$$
Z^{-1} X^{-1} Z X = \;\;\;\raisebox{-0.5em}{\includegraphics{fig}}\;\;\; = -1
\tag{4.15}
$$

Thus, there are two non-commuting operators acting on the ground state space $\mathfrak{L}$, and we conclude dim $\mathfrak{L} > 1$. In fact, there are four such operators, each of the two particle types can be moved around each of the two nontrivial cycles. Working out the commutation relations of these operators implies that dim $\mathfrak{L} = 4$.

4.3   The toric code in a field: perturbation analysis

We now apply a magnetic field to the toric code that will realistically allow the quasiparticles to hop and, unfortunately, destroy its exact solvability (see Tupitsyn *et al.* (2008)). To wit:

$$
H = -J_e \sum_s A_s - J_m \sum_p B_p - \sum_j \left(h_x \sigma_j^x + h_z \sigma_j^z \right)
\tag{4.16}
$$

For example, with $h_x = 0$ but $h_z \neq 0$, we can view the perturbation as an electric path operator of length 1 on each edge. Hence, it can cause charge pair creation and annihilation (at an energy cost $\sim 4J_e$) or hop existing charges by one lattice displacement, at no cost. For small h_z this provides a nontrivial tight-binding dispersion to the charges,

$$
\epsilon(q) \approx 2J_e - 2h_z (\cos q_x + \cos q_y)
\tag{4.17}
$$

but does not close the gap or lead to a change in the topological degeneracy of the ground state in the thermodynamic limit.

At large $h_z \gg J_e, J_m$, the model should simply align with the applied field as a paramagnet. Clearly, in this limit the topological degeneracy has been destroyed and we have a unique spin-polarized ground state. The phase transition can be understood
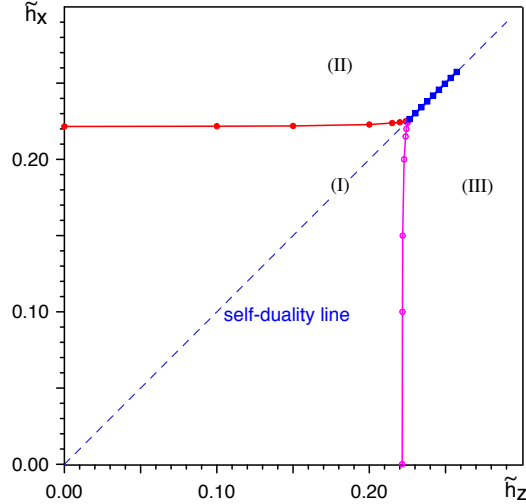
Fig. 4.1 Numerically determined phase diagram of the toric code in a field from Tupitsyn *et al.* (2008). (I) labels the topological phase, (II) and (III) the vortex and charge condensates (*i.e.* the paramagnetic phase). The numerics were done using discrete imaginary time with a rather large quantization step.

from the topological side as a bose condensation of the charges, which proliferate as h_z increases.

The same argument is applicable if $h_x \gg J_e, J_m$. If h_x increases while $h_z = 0$, then vortices condense. However, the high-field phase is just a paramagnet, so one can continuously rotate the field between the x- and z-direction without inducing a phase transition. Thus, the charge and vortex condensates are actually the same phase! This property was first discovered by Fradkin and Shenker (1979) for a 3D classical $\mathbb{Z}_2$ gauge Higgs model, where it appears rather mysterious.

4.4 Robustness of the topological degeneracy

The splitting of the ground state levels due to virtual quasiparticle tunneling is given by

$$\delta E \sim \Delta e^{-L/\xi} \tag{4.18}$$

This follows from the effective Hamiltonian

$$H_{\text{eff}} = -(t_{1Z} Z_1 + t_{2Z} Z_2 + t_{1X} X_1 + t_{2X} X_2) \tag{4.19}$$

where the Z_i, X_i operators are the winding loop operators of Sec. 4.2. Physically, this is simply a statement of the fact that the only way to act upon the ground state is to wind quasiparticles around the torus. This is a process exponentially suppressed in system size.

4.5 Emergent symmetry: gauge formulation

There are two ways to introduce symmetry operators in the perturbed toric code model.

1. One can define *loop operators* (e.g. Z_1, Z_2, X_1, X_2), the definition of which depends on the actual ground state of the perturbed Hamiltonian. This is similar to the definition of the operator Y in the 1D case of Sec. 2.5, which also requires detailed knowledge of the ground state.
2. One can exploit *gauge invariance* by rewriting the model in a gauge invariant form. This can be done for any spin model by introducing redundancy. In this case, the symmetry does not depend on the model but is only manifest in the topological phase.

We will take the second approach in order to avoid the difficulty of defining the appropriate loop operators and also to introduce the important gauge formulation of the model. To gauge the model we proceed in steps:

1. Introduce one extra spin μ_v per vertex that always remains in the state

$$\frac{1}{\sqrt{2}} \left(| \uparrow \rangle + | \downarrow \rangle \right).$$ (4.20)

This state is characterized by the condition

$$\mu_v^x |\Psi\rangle = |\Psi\rangle,$$ (4.21)

where μ_v^x is the Pauli spin matrix for the spin μ at vertex v.

2. Change spin operators from σ_{uv}, μ_v to $\tilde{\sigma}_{uv}, \tilde{\mu}_v$ where we represent the classical value of each old spin s_{uv} as $\tilde{m}_u \tilde{s}_{uv} \tilde{m}_v$. Here s_{uv} is the spin on the edge connecting u and v and m_u, m_v are the classical values of the new spins (*i.e.* the labels in the μ^z basis).

Thus the complete transformation is given by

$$\sigma_{uv}^z = \tilde{\mu}_u^z \tilde{\sigma}_{uv}^z \tilde{\mu}_v^z$$
$$\sigma_{uv}^x = \tilde{\sigma}_{uv}^x$$
$$\mu_u^z = \tilde{\mu}_u^z$$
$$\mu_u^x = \tilde{\mu}_u^x \prod_{j \in \text{star}(u)} \tilde{\sigma}_j^x = \tilde{\mu}_u^x \tilde{A}_u$$ (4.22)

and the constraint Eq. (4.21) becomes the standard $\mathbb{Z}_2$ gauge constraint:

$$\tilde{\mu}_u^x \tilde{A}_u |\Psi\rangle = |\Psi\rangle.$$ (4.23)

On states satisfying the gauge constraint Eq. (4.23), $A_u = \tilde{A}_u = \tilde{\mu}_u^x$. Therefore,

$$A_u |\Psi\rangle = \tilde{\mu}_u^x |\Psi\rangle$$ (4.24)

and we can rewrite the Hamiltonian as

$$H = -J_e \sum_v \tilde{\mu}_v^x - J_m \sum_p \tilde{B}_p - \sum_{\langle u,v \rangle} \left(h_x \tilde{\sigma}_{uv}^x + h_z \tilde{\mu}_u \tilde{\sigma}_{uv}^z \tilde{\mu}_v \right)$$ (4.25)

subject to the gauge constraint.

Viewed as a standard $\mathbb{Z}_2$ gauge theory, the protected topological degeneracy of the ground state is physically familiar as the protected degeneracy associated with the choice of flux threading the $2g$ holes of the genus g surface.
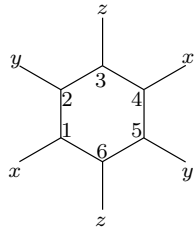
5
The honeycomb lattice model

We now investigate the properties of another exactly solvable spin model in two dimensions, the *honeycomb lattice model*. This model exhibits a number of gapped phases that are perturbatively related to the toric code of the previous sections. Moreover, in the presence of time-reversal symmetry breaking terms, a new topological phase arises with different topological properties, including nontrivial *spectral Chern number*. An extended treatment of the properties of this model with much greater detail can be found in Kitaev (2006).

In the honeycomb lattice model, the degrees of freedom are spins living on the vertices of a honeycomb lattice with nearest neighbor interactions. The unusual feature of this model is that the interactions are link orientation dependent (see Fig. 5.1). The Hamiltonian is

$$H = -J_x \sum_{x \text{ links}} \sigma_j^x \sigma_k^x - J_y \sum_{y \text{ links}} \sigma_j^y \sigma_k^y - J_z \sum_{z \text{ links}} \sigma_j^z \sigma_k^z \qquad (5.1)$$

We might expect this model to be integrable because $[H, W_p] = 0$ for an extensive collection of plaquette operators

$$W_p = \sigma_1^x \sigma_2^y \sigma_3^z \sigma_4^x \sigma_5^y \sigma_6^z$$
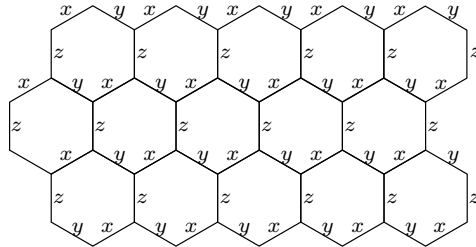
(5.2)

Fig. 5.1 The honeycomb model has spins living on the vertices of a honeycomb lattice with nearest neighbor interactions that are link-orientation dependent. x-links have $\sigma^x \sigma^x$ interactions, y-links have $\sigma^y \sigma^y$ interactions and z-links have $\sigma^z \sigma^z$ interactions.

where the spins and labels follow from the figure for each plaquette. Unfortunately, this is not quite enough: there are two spins but only one constraint per hexagon so that half of each spin remains unconstrained. In fact, the remaining degrees of freedom are Majorana operators!

5.1   A (redundant) representation of a spin by 4 Majorana operators

We consider a collection of four Majorana operators c, b^x, b^y and b^z that act on the 4-dimensional Fock space $\mathfrak{F}$. We define the following three operators

$$
\begin{aligned}
\tilde{\sigma}^x &= ib^x c \\
\tilde{\sigma}^y &= ib^y c \\
\tilde{\sigma}^y &= ib^y c.
\end{aligned}
\tag{5.3}
$$

These operators do not obey the spin algebra relations on the full Fock space, but we clearly have two extra dimensions of wiggle room. In fact, the physical state space is identified with a two-dimensional subspace $\mathfrak{L} \subset \mathfrak{F}$ given by the constraint

$$
D|\Psi\rangle = |\Psi\rangle, \quad \text{where } D = b^x b^y b^z c
\tag{5.4}
$$

Within $\mathfrak{L}$, the $\tilde{\sigma}^\alpha$ act as σ^α act on the actual spin. Of course, $\tilde{\sigma}^\alpha$ also act on $\mathfrak{L}^\perp$, but we can ignore these states by enforcing the constraint.

To be careful, we need to check two consistency conditions:

1. $\tilde{\sigma}^\alpha$ preserves the subspace $\mathfrak{L}$, which follows from $[\tilde{\sigma}^\alpha, D] = 0$.
2. The $\tilde{\sigma}^\alpha$ satisfy the correct algebraic relations when restricted to $\mathfrak{L}$. For example,

$$
\tilde{\sigma}^x \tilde{\sigma}^y \tilde{\sigma}^z = (ib^x c)(ib^y c)(ib^z c) = i^3(-1)b^x b^y b^z c^3 = iD = i
\tag{5.5}
$$

where the last equality only holds in the physical subspace $\mathfrak{L}$.

5.2   Solving the Honeycomb Model using Majoranas

We now use the Majorana representation of spins just introduced to rewrite each spin of the entire honeycomb model as in Fig. 5.2. This will greatly expand the 2^N-dimensional Hilbert space to the Fock space $\mathfrak{F}$ of dimension 2^{2N}, but the physical space $\mathfrak{L} \subset \mathfrak{F}$ is fixed by the gauge condition

$$
D_j|\Psi\rangle = |\Psi\rangle \quad \text{for all } j
\tag{5.6}
$$

where $D_j = b_j^x b_j^y b_j^z c$. We define a projector onto $\mathfrak{L}$ by

$$
\Pi_{\mathfrak{L}} = \prod_j \left(\frac{1 + D_j}{2} \right)
\tag{5.7}
$$

In the Majorana representation, the Hamiltonian (5.1) becomes

$$
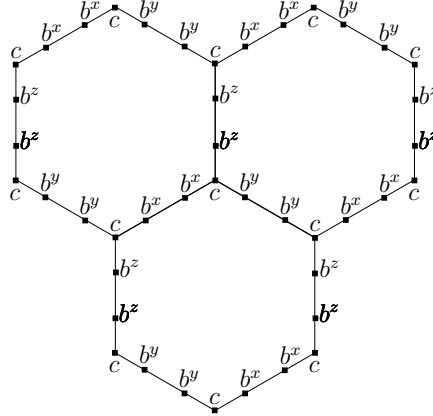\tilde{H} = \frac{i}{4} \sum_{\langle j,k \rangle} \hat{A}_{jk} c_j c_k
$$

Fig. 5.2 Majorana representation of honeycomb model.

$$\hat{A}_{jk} = 2J_{\alpha(j,k)}\hat{u}_{jk}$$
$$\hat{u}_{jk} = ib_j^{\alpha(j,k)}b_k^{\alpha(j,k)} \tag{5.8}$$

where $\alpha(j,k) = x, y, z$ is the direction of the link between j and k.

We have suggestively written the Hamiltonian $\tilde{H}$ as if it were a simple quadratic fermion Hamiltonian as in Sec. 2.4, but of course $\hat{A}_{jk}$ is secretly an operator rather than a real skew-symmetric matrix. However, each operator b_j^α enters only one term of the Hamiltonian and therefore $\hat{u}_{jk}$ commute with each other and with $\tilde{H}$! Thus, we can fix $u_{jk} = \pm 1$, defining an orthogonal decomposition of the full Fock space:

$$\mathfrak{F} = \bigoplus_u \mathfrak{F}_u, \quad \text{where } |\Psi\rangle \in \mathfrak{F}_u \text{ iff } \hat{u}_{jk}|\Psi\rangle = u_{jk}|\Psi\rangle \ \ \forall \, j, k \tag{5.9}$$

Within each subspace $\mathfrak{F}_u$, we need to solve the quadratic Hamiltonian

$$\tilde{H}_u = \frac{i}{4} \sum_{\langle j,k \rangle} A_{jk} c_j c_k$$
$$A_{jk} = 2J_{\alpha(j,k)}u_{jk} \tag{5.10}$$

which we know how to do in principle. On the other hand, the integrals of motion W_p (the hexagon operators) define a decomposition of the physical subspace $\mathfrak{L}$ labeled by the eigenvalues $w_p = \pm 1$:

$$\mathfrak{L} = \bigoplus_w \mathfrak{L}_w, \quad \text{where } |\Psi\rangle \in \mathfrak{L}_w \text{ iff } W_p|\Psi\rangle = w_p|\Psi\rangle \ \ \forall \, p \tag{5.11}$$

We can relate these two decompositions by expressing W_p in the Majorana representation and noting that within the physical subspace

$$\tilde{W}_p = \prod_{\langle j,k \rangle \in \partial p} \hat{u}_{jk} \tag{5.12}$$

Thus, we find

$$\mathfrak{L}_w = \Pi_\mathfrak{L}\mathfrak{F}_u \tag{5.13}$$

where $w_p = \prod_{(j,k)\in\partial p} u_{jk}$.

So we have a procedure for finding the ground state of the honeycomb model:

1. Fix $w_p = \pm 1$ for all p.
2. Find u_{jk} satisfying

$$w_p = \prod_{(j,k)\in\partial p} u_{jk}. \tag{5.14}$$

   There is a small subtlety here in that $u_{jk} = -u_{kj}$ so we must be careful about ordering. We can consistently take j in the even sublattice of the honeycomb and k in the odd sublattice in equation (5.14).
3. Solve for the ground state of the quadratic Hamiltonian (5.10), finding the energy $E(w)$.
4. Project the found state onto the physical subspace (*i.e.* symmetrize over gauge transformations).
5. Repeat for all w; pick the w that minimizes the energy.

If there were no further structure to $E(w)$, this would be an intractable search problem in the space of w_p. Fortunately, due to a theorem by Lieb (1994), the ground state has no vortices. That is,

$$E(w) = \min \text{ if } w_p = 1 \,\forall\, p \tag{5.15}$$

Using this choice of w_p, it is easy to solve the model and produce the phase diagram of Fig. 5.3. The gapless phase has two Dirac points in the fermionic spectrum.

5.3   Fermionic spectrum in the honeycomb lattice model

We just need to diagonalize the Hamiltonian

$$\tilde{H}_u = \frac{i}{4}\sum_{\langle j,k\rangle} A_{jk}c_j c_k$$

$$A_{jk} = 2J_{\alpha(j,k)}u_{jk}$$

$$u_{jk} = \begin{cases} +1 & \text{if } j \in \text{even sublattice} \\ -1 & \text{otherwise} \end{cases} \tag{5.16}$$

This is equivalent to finding the eigenvalues and eigenvectors of the matrix iA. Since the honeycomb lattice has two sites per unit cell, by applying the Fourier transform we get a 2×2 matrix $A(\vec{q})$:

$$iA(\vec{q}) = \begin{pmatrix} 0 & if(\vec{q}) \\ -if(\vec{q}) & 0 \end{pmatrix}$$

$$\epsilon(\vec{q}) = \pm|f(\vec{q})| \tag{5.17}$$

where $f(\vec{q})$ is some complex function that depends on the couplings J_x, J_y, J_z. In the gapless phase (phase B in Fig. 5.3), $f(\vec{q})$ has two zeros which correspond to Dirac points (see Fig. 5.4). At the transition to phase A, the Dirac points merge and disappear.
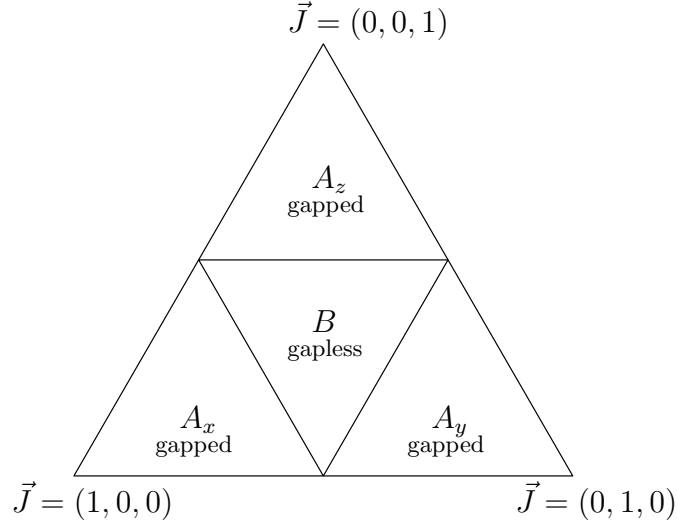
Fig. 5.3 Phase diagram of honeycomb model. This is a slice through the positive octant in $\vec{J}$ coupling space along the $J_x + J_y + J_z = 1$ plane. The other octants are analogous.

Fig. 5.4 Direct and reciprocal lattices of the honeycomb. The points $\pm\vec{q}_*$ are the two Dirac points of the gapless phase B.

5.4 Quasiparticle statistics in the gapped phase

It appears that there are two particle types: fermions and vortices (hexagons with $w_p = -1$). The vortices are associated with a $\mathbb{Z}_2$ gauge field, where u_{jk} plays the role of vector potential. Taking a fermion around a vortex results in the multiplication of the state by -1 (compared to the no-vortex case). However, the details such as the fusion rules are not obvious.

Let us look at the model from a different perspective. If $J_x = J_y = 0, J_z > 0$, the system is just a set of dimers (see Fig. 5.5). Each dimer can be in two states: $\uparrow\uparrow$ and $\downarrow\downarrow$. The other two states have $2J_z$ higher energy. Thus, the ground state is highly degenerate.

If $J_x, J_y \ll J_z$, we can use perturbation theory relative to the noninteracting dimer point. Let us characterize each dimer by an effective spin:

$$| \Uparrow \rangle = | \uparrow\uparrow \rangle; \qquad | \Downarrow \rangle = | \downarrow\downarrow \rangle. \tag{5.18}$$

At 4th order of perturbation theory, we get:

$$H_{\text{eff}}^{(4)} = \text{const} - \frac{J_x^2 J_y^2}{16 J_z^3} \sum_p Q_p \tag{5.19}$$
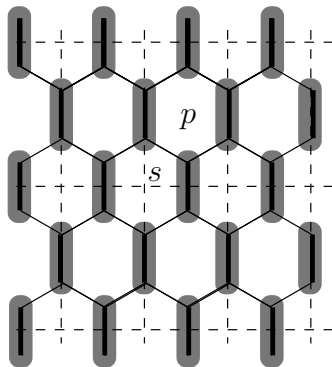
Fig. 5.5 The vertical dimers on the honeycomb lattice themselves form the edges of a (dashed) square lattice. The plaquettes of alternate rows of the hexagonal lattice correspond to the stars and plaquettes of the square lattice. This is *weak breaking of translational symmetry.*

where p runs over the square plaquettes of the dimer lattice (see Fig. 5.5) and

$$Q_p = \sigma^y_{p_1} \sigma^x_{p_2} \sigma^y_{p_3} \sigma^x_{p_4} \tag{5.20}$$

is a plaquette operator on the effective spin space $| \Uparrow \rangle$, $| \Downarrow \rangle$. By adjusting the unit cell and rotating the spins, we can reduce this Hamiltonian to the toric code!

The vertices and plaquettes of the new lattice correspond to alternating rows of hexagons. Thus, vortices on even rows belong to one superselection sector and vortices on odd rows to the other. It is impossible to move a vortex from an even row to an odd row by a local operator without producing other particles (*e.g.* fermions). The fermions and $e - m$ pairs belong to the same superselection sector, ϵ, though these are different physical states.

5.5 Nonabelian phase

In the gapless phase B, vortex statistics are not well-defined. However, a gap can be opened by applying a perturbation that breaks the time-reversal symmetry, such as a magnetic field. Unfortunately the honeycomb model in a field is not exactly solvable. Yao and Kivelson (2007) studied an exactly solvable spin model where the time-reversal symmetry is spontaneously broken, but we will satisfy ourselves by introducing a T-breaking next nearest neighbor interaction on the fermionic level (which can be represented by a 3-spin interaction in the original spin language).

Written in terms of Majorana fermions, we consider the Hamiltonian

$$H = \frac{i}{4} \sum_{\langle j,k \rangle} A_{jk} c_j c_k \tag{5.21}$$

where A_{jk} now has chiral terms connecting Majoranas beyond nearest neighbor in the honeycomb lattice (see Fig. 5.6). After Fourier transforming, we find
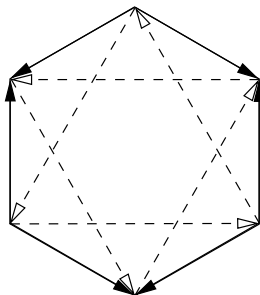
Fig. 5.6 Picture of chiral interaction matrix A_{jk}. Forward arrows correspond to positive entries in the skew-symmetric real matrix A_{jk}. Solid arrows are the interactions of the original honeycomb model; dashed arrows give the time-reversal symmetry breaking perturbation.

$$iA(\vec{q}) = \begin{pmatrix} \Delta(\vec{q}) & if(\vec{q}) \\ -if(\vec{q}) & -\Delta(\vec{q}) \end{pmatrix} \tag{5.22}$$

with the massive dispersion relation

$$\epsilon(\vec{q}) = \pm\sqrt{f(\vec{q})^2 + \Delta(\vec{q})^2}. \tag{5.23}$$

Within this massive phase, we will find nontrivial topological invariants of the quasiparticle spectrum. Let $iA(\vec{q})$ be a nondegenerate Hermitian matrix that continuously depends on $\vec{q}$. In our case, A acts in $\mathbb{C}^2$, but in general it can be $\mathbb{C}^n$ for any n. Let us keep track of the "negative eigenspace" of $iA(\vec{q})$: the subspace $\mathfrak{L}(\vec{q}) \subseteq \mathbb{C}^n$ spanned by eigenvectors corresponding to negative eigenvalues. For matrix (5.22), dim $\mathfrak{L}(\vec{q}) = 1$. This defines a map F from momentum space (the torus) to the set of m-dimensional subspaces in $\mathbb{C}^n$. More formally:

$$F: \ \mathbb{T}^2 \longrightarrow U(n)/U(m) \times U(n-m) \tag{5.24}$$

This map F may have nontrivial topology.

In the honeycomb model with T-breaking, we have $n = 2$, $m = 1$ and $U(2)/U(1) \times U(1) = \mathbb{C}P^1 = S^2$ is the unit sphere. Thus, $F : \mathbb{T}^2 \longrightarrow S^2$ and for the matrix $iA(\vec{q})$ of Eq. (5.22), F has degree 1. That is, the torus wraps around the sphere once. More abstractly, $\mathfrak{L}(\vec{q})$ defines a complex vector bundle over the momentum space $\mathbb{T}^2$. This has an invariant Chern number ν, which in this case is $\nu = 1$.

What is the significance of the spectral Chern number? It is known to characterize the integer quantum Hall effect, where it is known as the "TKNN invariant". For a Majorana system, there is no Hall effect since particles are not conserved. Rather, the spectral Chern number determines the number of chiral modes at the edge:

$$\nu = (\# \text{ of left-movers}) - (\# \text{ of right-movers}). \tag{5.25}$$

5.6 Robustness of chiral modes

A chiral edge mode may be described by its Hamiltonian:

$$H_{\text{edge}} = \frac{iv}{4} \int \hat{\eta}(x)\partial_x\hat{\eta}(x)dx \qquad (5.26)$$

where $\hat{\eta}(x)$ is a real fermionic field. That is,

$$\hat{\eta}(x)\hat{\eta}(y) + \hat{\eta}(y)\hat{\eta}(x) = 2\delta(x - y). \qquad (5.27)$$

At temperature T, each mode carries energy current

$$I_1 = \frac{\pi}{24}T^2. \qquad (5.28)$$

The easiest explanation of this is a straightforward 1-D fermi gas calculation:

$$\begin{aligned}
I_1 &= v \int_0^\infty n(q)\epsilon(q)\frac{dq}{4\pi} \\
&= \frac{1}{2\pi} \int_0^\infty \frac{\epsilon d\epsilon}{1 + e^{\epsilon/T}} \\
&= \frac{\pi}{24}T^2
\end{aligned} \qquad (5.29)$$

However, it is useful to reexamine this current using conformal field theory (CFT), in order to understand better why the chiral modes are robust. We consider a disc of B phase extended into imaginary time at temperature T. That is, we have a solid cylinder with top and bottom identified:
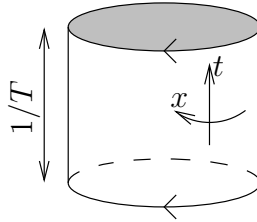
We have obtained a solid torus whose surface is a usual torus. The partition function is mostly determined by the surface.

Let the spatial dimensions be much greater than $\frac{1}{T}$. From this point of view, the cylinder looks more like:

According to the usual CFT arguments, we have

$$Z \sim q^{\frac{c}{24}}\bar{q}^{\frac{\bar{c}}{24}}$$

$$q = e^{2\pi i \tau}$$

$$\tau = i\frac{LT}{v} + \text{twist} \tag{5.30}$$

Twisting the torus changes the partition function by:

$$\tau \mapsto \tau + 1$$

$$Z \mapsto Z e^{2\pi i \frac{c-\bar{c}}{24}}. \tag{5.31}$$

On the other hand, the twist parameter $(\text{Re}\,\tau)$ couples to the some component of the energy-momentum tensor, namely, T_{xt}, which corresponds to the energy flow. This relation implies that

$$I = \frac{\pi}{12}(c - \bar{c})T^2. \tag{5.32}$$

The chiral central charge, $c - \bar{c}$, does not depend on the boundary conditions. Indeed, the energy current on the edge cannot change because the energy cannot go into the bulk.

References

Einarsson, T. (1990). Fractional statistics on a torus. *Phys. Rev. Lett.*, **64**(17), 1995–1998.

Fradkin, E. and Shenker, S. H. (1979). Phase diagrams of lattice gauge theories with higgs fields. *Phys. Rev. D*, **19**(12), 3682–3697.

Hastings, M. B. and Wen, X. G. (2005). Quasiadiabatic continuation of quantum states: The stability of topological ground-state degeneracy and emergent gauge invariance. *Phys. Rev. B*, **72**(4), 045141.

Kitaev, A. (2000). Unpaired majorana fermions in quantum wires. *arXiv*, **cond-mat/0010440v2**.

Kitaev, A. (2003). Fault-tolerant quantum computation by anyons. *Ann. Phys.*, **303**(1), 2 – 30.

Kitaev, A. (2006). Anyons in an exactly solved model and beyond. *Ann. Phys.*, **321**(1), 2 – 111.

Lieb, E. H. (1994). Flux phase of the half-filled band. *Phys. Rev. Lett.*, **73**(16), 2158–2161.

Read, N. and Chakraborty, B. (1989). Statistics of the excitations of the resonating-valence-bond state. *Phys. Rev. B*, **40**(10), 7133–7140.

Tupitsyn, I. S., Kitaev, A., Prokof'ev, N. V., and Stamp, P. C. E. (2008). Topological multicritical point in the toric code and 3d gauge higgs models. *arXiv*, **0804.3175v1**.

Yao, H. and Kivelson, S. A. (2007). Exact chiral spin liquid with non-abelian anyons. *Phys. Rev. Lett.*, **99**(24), 247203.